Illite–Smectite Mixed-Layer Minerals in the Alteration Volcanic Ashes Under Submarine Environment

Hanlie Hong, Wenpeng Gao, Ke Yin, Zhaohui Li, and Chaowen Wang

Abstract The clay mineralogy of the clay intervals interbedded with siliceous mudstones across the Permian–Triassic boundary (PTB) in Pengda, Guiyang, Guizhou province, was investigated by X-ray diffraction (XRD) and high-resolution transmission electron microscopy (HRTEM). The clay mineral assemblages of the sediments are mainly I/S clays and minor smectite, kaolinite, and illite as revealed by XRD analyses. The peak-shaped parameters BB1 and BB2 of I/S clays of the representative clay bed PL-01 are 4.7° and 4.4°, respectively, and the peak position of the low-angle diffraction is at 6.5° 2θ (13.6 Å), suggesting that the I/S clays have a IS type of ordering. However, multi-order diffractions and their intensities are different from those of completely ordered 1:1 mixed-layer I/S clay rectorite, indicating that I/S clays of the Pengda section have partially ordered IS structures. HRTEM observations show that most of the I/S clays exhibit a IS stacking ordering. However, in some areas within a IS particle, smectite layer is observed in doublets, triplets, and quartets, which are interstratified by various amounts of illite layers, suggesting the presence of other irregular stacking in addition to the major 1:1 IS-ordered stacking. Transformation of smectite layer into illite layers is also observed in the I/S clays, suggesting that the Pengda I/S clays are derived from smectite illitization, in good agreement with the clay mineral assemblage. The I/S clays of the Pengda section contain up to 45–95 % smectite layer, the notably higher contents of smectite layer relative to those of other PTB stratigraphic sets in south China can be attributed to the difference in alteration and smectite illitization processes due to different sedimentary environments.

Keywords Permian–Triassic boundary (PTB) • High-resolution transmission electron microscopy (HRTEM) • Clay minerals • Mixed-layer illite–smectite

H. Hong (✉) • W. Gao • K. Yin • C. Wang
Faculty of Earth Sciences, China University of Geosciences, Wuhan, Hubei 430074, People's Republic of China
e-mail: hongh18311@yahoo.com.cn

Z. Li
Faculty of Earth Sciences, China University of Geosciences, Wuhan, Hubei 430074, People's Republic of China

Geosciences Department, University of Wisconsin—Parkside, Kenosha, WI 53141-2000, USA

F. Dong (ed.), *Proceedings of the 11th International Congress for Applied Mineralogy (ICAM)*, Springer Geochemistry/Mineralogy,
DOI 10.1007/978-3-319-13948-7_15

1 Introduction

The Permian–Triassic boundary (PTB) mass extinction is considered as the most serious biotic crisis in the history of life, in which both marine and terrestrial biota suffered near annihilation [1, 2]. The causes for this biotic crisis are still debated [3]. However, the pronounced and worldwide negative carbon isotope excursion at the PTB is indicative of a strong disruption in carbon reservoirs [2, 4], related to prominent volcanic events of the Siberian Traps [3, 5, 6]. In the PTB stratigraphic set in south China, there occur several clay intervals with a thickness of mainly 2–20 cm interbedded within carbonate sediments that encompass mass extinction. These intervals were recognized as products of alteration of volcanic ashes based on the associated heavy minerals and clay mineral composition. Previous studies on the PTB clay intervals were focused mainly on mineral composition, clay morphology, and their provenance [7–11]. The identification of clay minerals from XRD measurement suggests that mixed-layer I/S clays dominantly comprise the clay sediments, but the stacking structures of the mixed-layer I/S clays are still not well known [11–14], making it difficult to reveal the formation of clays in the sediments due to alteration and transformation between clay minerals during diagenesis.

XRD measurement provides usually the information on average layer stacking of mixed-layer I/S clays within crystallites based on Markovian statistics, while HRTEM analysis gives structural information on layer stacking in local regions within a crystallite. For investigation of the transformation mechanisms of I/S clays during diagenesis, HRTEM methods have been utilized to determine the structures of mixed-layer I/S minerals [15–17]. The clay beds within the PTB stratigraphic set in south China provide an opportunity to study the formation of mixed-layer I/S minerals resulted from the alteration of volcanic ashes under submarine environment. However, only rare HRTEM study was undertaken to investigate their transformation mechanisms. In this study, we investigated the one-dimensional structure images of mixed-layer I/S minerals using HRTEM analysis in combination with XRD analyses to obtain a better understanding of clay mineralogical characteristics and formation mechanisms of I/S minerals from the alteration of volcanic ashes under submarine environment.

2 Materials and Methods

2.1 Sample Preparation

The Pengda section (26.37°N, 106.59°E) is located at Dangwu town, Guiyang city, Guizhou province, southeastern China. A general map of the study area around Guiyang is shown in Fig. 1. In the PTB stratigraphic set, there are eight clay layers each with a thickness of 3–12 cm interbedded with siliceous mudstones, based on their distinctive color, texture, and composition. The siliceous mudstones are

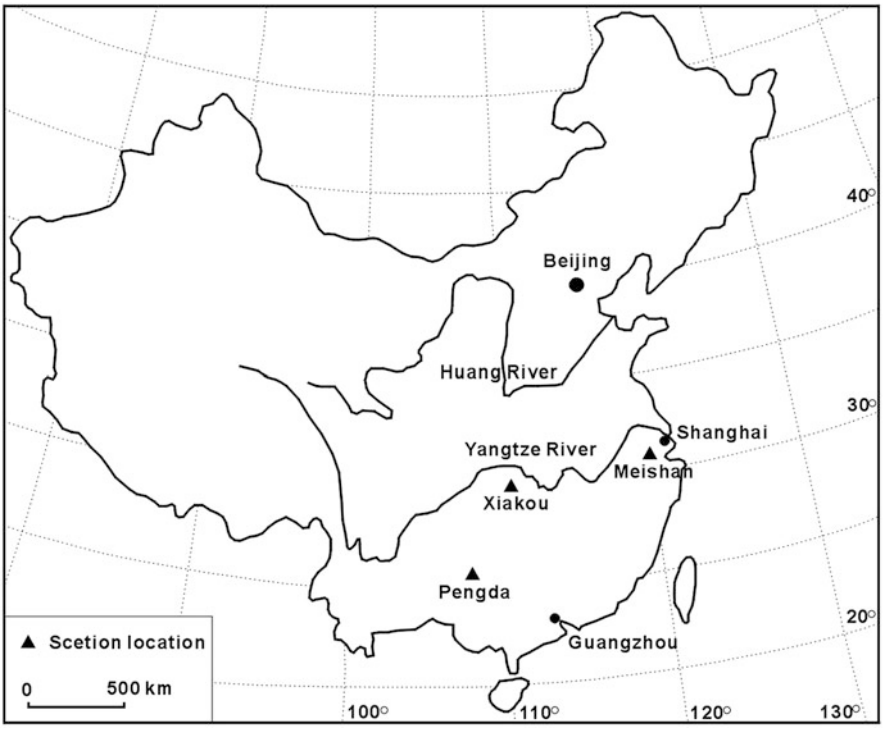

Fig. 1 A generalized map showing the location of the PTB sections

considered as neritic deposits according to the occurrence of Radiolaria fossils [18]. Representative clay samples, weighing around 500 g, were collected from each of the eight interbedded clay layers across the PT boundary according to their distinctive color, texture, and composition.

2.2 XRD Analysis

Bulk clay samples were air dried and then crushed and ground to powder with a pestle and mortar, and the clay–mineral fraction was obtained by the sedimentation method as described by Jackson [19]. Oriented clay samples were prepared by carefully pipetting the clay suspension on a glass slide and were air dried at ambient temperature. Ethylene glycol saturated clays were prepared by vapor treatment method. The oriented clay samples were placed on the shelf of a desiccator with about 1 cm depth of ethylene glycol in the base, which was then placed in an oven and saturated at 65 °C for about 4 h. The XRD patterns were recorded from 3° to 65° 2θ at a scan rate of 4° 2θ/min using a Rigaku D/MAX-IIIA diffractometer, with

Ni-filtered Cu Kα radiation (1.5404 Å) and 1° divergence slit, 1° anti-scatter slit, and 0.3 mm receiving slit.

Clay species were identified by their characteristic diffractions, as discussed by Moore and Reynolds [20]. Illite was identified using its 001 diffraction of 10 Å spacing. Smectite was identified by the 15-Å diffraction at air-dried conditions. Mixed-layer illite–smectite has the basal 001 spacing of 10–15.5 Å, and was further identified by their glycolated samples. The basal 001 diffraction of glycolated chlorite is 14 Å and the 001 and 002 diffractions of kaolinite are 7.15 and 3.57 Å, respectively.

The relative proportions of clay minerals in the sample were estimated using the weighting factor method [21, 22]. Semiquantitative calculation of the clay phases was undertaken in the air-dried sample, for the 001 diffraction of I/S clays separates into two peaks with varied intensity ratios among the samples after glycolated treatment, due to the difference in illite and smectite layer contents between the I/S clays. The weighing factors were adopted from Hong et al. [14] and Schwertmann and Niederbudde [23], which are 7.5, 5.0, 1.0, 1.0, and 1.3 for I/S clay, illite, smectite, kaolinite, and chlorite, respectively. The detection limits were 1 % for kaolinite, smectite, and chlorite, 3 % for illite, and ~5 % for mixed-layer I/S.

Percentages of smectite layers in I–S were estimated using the reciprocal vector method [12], which was calculated using the formula: $1/d001(I/S) = \alpha/d001(I) + \beta/d001(S)$, where d001(I/S) is the d-spacing of the 001 diffraction of the mixed-layer I/S, and d001(I) and d001(S) are those of the 001 diffractions of illite and smectite, with *d* values of 10 and 15.5 Å, respectively, and α and β represent the layer content of illite and smectite in the mixed-layer I/S with the relation $\alpha + \beta = 1$.

2.3 HRTEM Analysis

A clay fraction separated from bed PL-01 was selected as the representative sample in our HRTEM analysis. The air-dried clay fraction was embedded in M-bond 610 resin and was then placed between two Si slides and allowed to solidify in an electric oven at 80 °C for ~2 h. The resin-solidified clay sample was cut vertically so that the (001) planes of clay particles were perpendicular to the cut surface. The thin slices were further thinned to ultrathin sections with a thickness <50 nm using ion-beam thinning techniques. HRTEM analysis was performed on a Philips CM12 high-resolution transmission electron microscope equipped with an EDAX9100 X-ray energy-dispersive detector (EDS), which was operated at an accelerating voltage of 120 kV and a beam current of ~20 nA. The lattice-fringe images of clay minerals were taken under over-focus conditions [24], for this condition usually gives the best contrast effect of the mixed-layer clay minerals. The point and line resolutions were 0.34 nm and the 0.20 nm respectively.

3 Results

3.1 Clay Mineralogy of the Pengda Clay Beds

The XRD patterns of the air-dried and glycolated clay fractions are shown in Fig. 2. Most of the air-dried samples display a strong peak of 11–15 Å, and some of the samples exhibit two peaks, one has the *d*-value of ~15 Å and another has the *d*-value of 12–14 Å. Glycolated treatment of the air-dried samples with a strong peak produces two separate peaks in this region, one at ~16.7 Å and one at 9.0–9.5 Å. Ethylene glycol saturation of the air-dried samples with two peaks produces three separate peaks at 16.7, ~13.6, and ~9.3 Å, respectively. These suggest that smectite and I/S clays are the dominant clay components in the samples. The weak 7.15 Å peak is present in all samples, indicating that kaolinite occurs as a minor component in all the clay sediments.

Samples PL-02 and PL-03 are composed dominantly of I/S clays and minor kaolinite, while samples PL-01, PL-04, PL-05, and PL-06 consisted of mainly I/S clays and contain small amounts of smectite and kaolinite. In addition, the XRD profiles reveal that chlorite is only present in sample PL-07 as a minor component, which is not detected in other samples. Calculations from the XRD patterns of the air-dried clay fractions show that the I/S clays contain varying amounts of smectite layers. I/S clays of Layer PL-02 contain up to 95 % smectite layers, while PL-06 has only 45 % smectite layers.

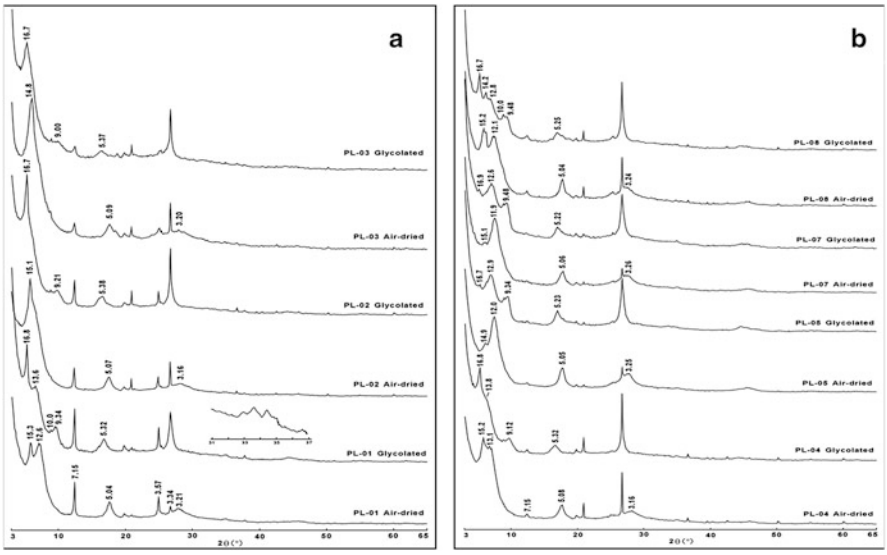

Fig. 2 XRD patterns of air-dried and glycolated clays from the Pengda section. (**a**) Beds PL-01–PL-03; (**b**) Beds PL-04–PL-07

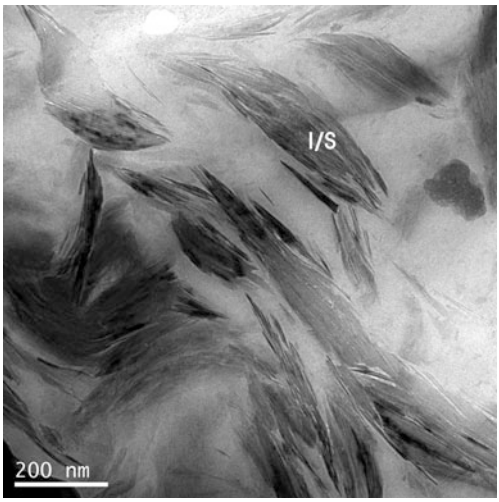

Fig. 3 The HRTEM image shows the typical wave-shaped morphology of the Pengda I/S clays

3.2 Layer Stacking of I/S Clays

Observations on the air-dried samples showed that most clay particles exhibit typical wave-shaped morphology with only trace in straight outline (Fig. 3), suggesting that clay minerals are mainly I/S clays and smectite [25], in agreement with the results from XRD analysis. In general, crystal boundaries of the clay particles could be readily recognized and the lattice fringes bent but well defined.

The I/S clays are characterized by lattice-fringe spacings of interstratified 10 and 12 Å under HRTEM observation. Some wave-shaped particles appear to have 12 Å fringes only, without or with only few interstratified 10 Å layers, while in most of the clay particles the lattice fringes consist of mainly 10 Å layers and minor 12 Å layers (Fig. 4a–c). The former may be interpreted as smectite phase and the latter as I/S clays, for the 15 Å smectite lattice-fringe spacing collapsed to 12 Å under the electron beam [26]. In most particles, the interstratified illite/smectite sequences are ordered and exhibit a layer proportion of 1:1 (Fig. 4a). In some particles, the 10 Å illite layers are interstratified with 12 Å smectite layers, and the illite/smectite sequences are disordered. Smectite layer is present in units of doublets, triplets, and quartets, which are interstratified by various amounts of illite layers (Fig. 4b). In some regions of the lattice-fringe image, one smectite layer laterally split into two illite layers (Fig. 4c), suggesting the transformation of smectite into I/S clays.

In some small particles, the lattice fringes are straight and are all 10 Å thick (Fig. 4a), indicative of illite mineral. The EDS analyses of clay particles show that their elemental composition consists of mainly Si, Al, and minor K, Ca, Na, Mg, and Fe. However, the areas with mainly 12 Å lattice-fringe spacings contain more Na and Mg, confirming the presence of a smectite mineral, while the areas with mainly 10 Å lattice-fringe spacings have more K but less Ca and Mg, indicating the presence of an illite mineral.

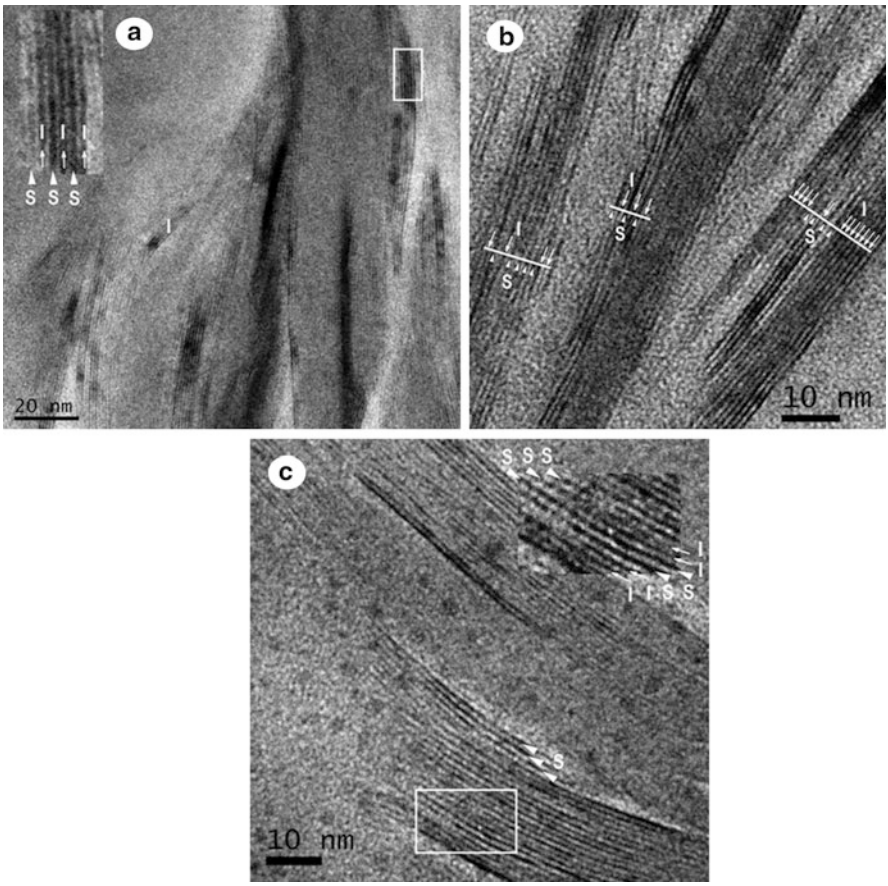

Fig. 4 Lattice-fringe images of the I/S clays. (**a**) 1:1 IS stacking ordering; (**b**) smectite layer in doublets, triplets, and quartets, interstratified by various amounts of illite layers; (**c**) the lateral transition S → I. *I* illite layer, *S* smectite layer

4 Discussion

4.1 Characteristics of Pengda I/S Clays

The characteristic diffraction of the air-dried I/S clay is 12.6 Å and that of its glycolated product is 13.6 Å, which are quite similar to the ordered 1:1 mixed-layer I/S clay rectorite [27, 28]. The structure of I/S clays could be determined using the two noncoincident mixed-layer diffractions at 6–8° and 33–35° 2θ [29]. The peak-shaped parameters BB1 (angle width of the complex 10 Å diffraction) and BB2 (angle width of the diffraction at 33–35°) measured from the XRD pattern of glycolated sample are 4.7° and 4.4°, respectively, which are larger than the criteria value of >4.0° for ordering IS clay, suggesting that the I/S clay in layer PL-01 of the

Pengda section has an IS type of ordering. This is also confirmed by the peak position of the low-angle diffraction at 6.5° (the criteria value of <7.5°) [29].

The ordering types of I/S clays are also correlated with the smectite contents of the I/S minerals. For I/S clays with ~50 % smectite layers, their interstratification structures vary from completely random to maximum IS ordered, and change in content of smectite layer will favor the occurrence of partially ordered IS structures [30]. For the perfectly ordered 1:1 mixed-layer I/S clay rectorite and its glycolated product, almost all theoretically multi-order diffractions of 001 could be observed in their XRD patterns. However, unlike those of rectorite, only 12.6, 5.05, 3.17, 2.57, and 1.99 Å diffractions of the air-dried sample and 13.6, 9.34, 5.32, 3.33, 2.56, and 2.03 Å diffractions of the glycolated sample could be observed in their XRD patterns of the Pengda I/S clay. The peaks are relatively broad and their intensities are relatively weak. Again, at the low-angle side of 2.56 Å peak there is a diffuse band at ~33° 2θ, suggesting the occurrence of certain amounts of random interstratification I/S clays [29]. Therefore, the I/S clay of layer PL-01 in the Pengda section consists of mainly IS ordering mineral and randomly interstratified I/S mineral as indicated by the XRD analysis.

Illitization process and the crystal chemistry of I/S depend on environmental conditions, such as temperature, compositions of fluid and rock and water/rock ratio, as well as geological time. Variability in the inherited characteristics of smectite formed during earlier periods of alteration may also influence later illitization during burial diagenesis. HRTEM observations show that most of the I/S clays exhibit an IS stacking ordering, in agreement with the results of XRD analysis. However, in local regions within a crystallite, the IS layer stacking sequences are irregular. Smectite layers are observed in layer-doublets, layer-triplets, and layer-quartets, which are interstratified by various amounts of illite layers. These suggest that the stacking of Pengda I/S clay consists of various types of the subunits, in addition to the 1:1 IS-ordered stacking, and the smectite illitization can be described by a systematic change in the type and proportion of the subunits constituting crystallites [31]. Transformation of the smectite layer into illite layers in HRTEM observations reinforces the hypothesis that the Pengda I/S clays are derived from smectite illitization.

4.2 Formation of Clay Beds in the Pengda Section

In diagenesis processes, discrete clay minerals are little changed and the main change in clay mineralogy is an increase in the amounts of illite layers together with the increasing degree of ordering of I/S clays [32, 33]. However, in the Pengda section, the I/S clays containing a large amount of smectite layers (Beds PL-02 and PL-03) are interbedded with those having relatively smaller amount of smectite layers (Beds PL-01 and PL-04). The transformation of smectite to illite often takes place at the temperature of oil formation during burial diagenesis [34]. The PTB

stratigraphic set in south China is mature for oil generation [35]. It would be expected that the I/S clays in the Pengda have undergone smectite illitization and an increase in ordering in the layer-type distribution. However, these clay beds occur only within 3 m thick sediments, the difference in amount of smectite layer in the I/S clays should not be attributed to different burial temperatures. Variation in the amount and type of discrete clay minerals between the clay beds can be attributed to different parent materials and the environment conditions of the episode of volcanism.

Though the clay sediments are recognized as an alteration product of volcanic ashes, and in one case as a mixture of volcaniclastic and continental alteration materials [14], the sedimentary environment and the redox conditions may be different between the volcanism episodes, as suggested by the differences in color, texture, and mineralogical characteristics of the clay sediments. The variation in color from pale yellow to dark gray may probably reflect increasingly reducing conditions, and changes in texture and clay mineral composition may be derived from sedimentation rate and chemical composition of the parent volcanic ashes. Thus, variations in the amount of smectite layers in the I/S clays of the clay sediments could be due to different parent materials [36]. The occurrence of chlorite and illite, in association with larger amount of I/S clays in the clay beds, is indicative of a mixture of terrigenous and volcanic sources, similar to those found in other PTB stratigraphic sets elsewhere in south China [14].

Kaolinite is usually considered as a result of intense chemical weathering [37]. However, authigenic kaolinite could also be formed in early diagenesis in a relatively acid environment. The PTB stratigraphic set at Pengda consists of mainly siliceous mudstones with interbedded clay beds; in early diagenesis, the contact with acid siliceous deposits could have caused the removal of alkali elements in solution and resulted in the formation of kaolinite [38]. The interbedded pure smectite beds in marine sediments are usually derived from marine alteration of volcanic ashes [25, 39–41], and the major mineral I/S could represent a major smectitic volcanogenic component that was converted to I/S by alteration [25, 40, 42, 43]. XRD results show that clay beds in the Pengda section are composed of mainly I/S clays, smectite, and minor kaolinite and illite, which are considered as alteration products of volcanic ashes in marine environment in association with the alteration of burial diagenesis. Dong et al. [16] suggested that smectite illitization produces mainly I/S clays with small proportions of smectite and illite. The major mineral I/S clays in association with minor smectite and illite in the Pengda section may probably reflect the transformation of smectite to illite, as is confirmed by HRTEM observations.

Clay mineral assemblages of the Pengda clay beds are mainly I/S clays, smectite, and kaolinite, and the I/S minerals in this section contain up to 45–95 % smectite layers (Table 1). However, clay minerals of the Meishan section consist mainly of I/S clays, illite, and kaolinite, with 27–50 % smectite layers within the I/S clays, and clay minerals of the Xiakou section are composed of only I/S clays, with only 15–31 % smectite layers [14]. The smectite layer contents of I/S clays in the Pengda section are significantly higher than those in the Xiakou, Meishan, and many other

Table 1 Clay mineral compositions of clay intervals in the Pengda PTB stratigraphic set (vol%)

Layer	Color and texture	I/S	Smectite	Kaolinite	Illite	Chlorite	S content in I/S (%)
PL-01	Grayish white, loose	78	8	9	5	–	58
PL-02	Grayish white, condensed	93	–	4	3	–	95
PL-03	Light gray to pale yellow, condensed	90	–	3	7	–	91
PL-04	Dark gray, loose	81	11	3	5		67
PL-05	Grayish yellow to grayish green, loose	87	3	1	9	–	47
PL-06	Grayish yellow to grayish green, loose	88	2	2	8	–	45
PL-07	Dark gray, condensed with lamination	62	9	3	16	10	49

sections [10, 14]. Unlike the Pengda section formed in neritic sea environment, the Meishan sediments formed in an intraplatform depression between an uplift and a platform, and the Xiakou deposits formed in an open continental-shelf sedimentary environment [44, 45]. Variations in clay assemblage and smectite layer content of the I/S clays among the PTB stratigraphic sets can be attributed to different sedimentary environment, which may have resulted in differences in redox and weathering conditions and in alteration processes during burial diagenesis.

5 Conclusions

The clay intervals with siliceous mudstones across the PT boundary in the Pengda section consist mainly of I/S clays with minor kaolinite, smectite, and illite. Chlorite only occurs in layer PL-07, though the peak-shaped parameters BB1 and BB2 of I/S clays of layer PL-01 are 4.7° and 4.4°, respectively, suggesting that the I/S clays has an IS type of ordering, as is also confirmed by the peak position of the low-angle diffraction at 6.5°2θ (13.6 Å). The presence of multi-order diffraction and their intensities is different from those of completely ordered 1:1 mixed-layer I/S clay rectorite, suggesting that I/S clays of the Pengda section have partially ordered IS structures.

Most of the I/S clays exhibit an IS stacking ordering under HRTEM observations. However, in some areas within an IS particle, smectite layer is present as units of doublets, triplets, and quartets, which are interstratified by various amounts of illite layers. These reinforce that the stacking of Pengda I/S clays consists of various types of the subunits, in addition to the major 1:1 IS-ordered stacking, in good agreement with the results of XRD analysis. Transformation of the smectite layer into illite layers is also observed under HRTEM observations, confirming that

the Pengda I/S clays are derived from smectite illitization. I/S clays of the Pengda section contain up to 45–95 % smectite layers, which are notably higher than those of other sections in south China, such as the Meishan section (27–50 %) and the Xiakou section (15–31 %). Variations in smectite layer content of the I/S clays among the PTB stratigraphic sets may reflect the differences in alteration and smectite illitization processes due to the different sedimentary environments.

Acknowledgment This work was supported by the Natural Science Foundation of China (41272053 and 41072030) and the Specialized Research Fund for the Doctoral Program of Higher Education of China (20110145110001). The authors wish to thank Jiang H. S. for sample preparations, Dr. Liu X. W. for HRTEM observations, and Dr. Yu J. S. for XRD analyses, and especially Prof. Dong F. Q. and Zhao X. Q., the Guest Editors, and two anonymous reviewers for their insightful reviews, valuable comments, and suggestions.

References

1. Erwin DH (1994) The Permo-Triassic extinction. Nature 367:231–236
2. Jin YG, Wang Y, Wang W, Shang QH, Cao CQ, Erwin DH (2000) Pattern of marine mass extinction near the Permian-Triassic boundary in south China. Science 289:432–436
3. Korte C, Kozur HW (2010) Carbon-isotope stratigraphy across the Permian-Triassic boundary: a review. J Asian Earth Sci 39:215–235
4. Holser WT, Schölaub HP, Attrep M, Boeckelmann K, Klein P, Magaritz M, Orth CJ, Fenninger A, Jenny C, Kralik M, Mauritsch H, Pak E, Schramm JM, Stattegger K, Schmöler R (1989) A unique geochemical record at the Permian/Triassic boundary. Nature 337:39–44
5. Wignall PB (2001) Large igneous provinces and mass extinctions. Earth Sci Rev 53:1–33
6. Knoll AH, Bambach RK, Payne JL, Pruss S, Fischer WW (2007) Paleophysiology and end-Permian mass extinction. Earth Planet Sci Lett 256:295–313
7. Wu SB, Ren YX, Bi XM (1990) Volcanic material and origin of clay rock near Permo-Triassic boundary from Huangshi, Hubei and Meishan of Changxing county, Zhejiang. Earth Sci J China Univ Geosci 15:589–594
8. Lu Q, Lei XR, Liu HF (1991) Genetic types and crystal chemical classification of irregular illite/smectite interstratified clay minerals. Acta Mineral Sin 11:97–104, Chinese text with English abstract
9. Yin HF, Huang SJ, Zhang KX, Hansen HJ (1992) The effects of volcanism on the Permo-Triassic mass extinction in South China. In: Sweet WC, Yang ZY, Dickins JM, Yin HF (eds) Permo-Triassic events in the eastern Tethys. Cambridge University Press, Cambridge, pp 146–157
10. Zhang SX, Yu JX, Yang FQ, Peng YQ, Yin HF, Yu JS (2004) Study on clayrocks of the neritic, littoral and marine-terrigenous facies across the permiantriassic boundary in the eastern Yunnan and western Guizhou, south China. J Mineral Petrol 24:81–86, Chinese text with English abstract
11. Yu KP, Han GM, Yang FL, Mansy JL, Xu CH, Zhou ZY, Cheng XR, Liu ZF, Fu Q (2005) Study on clay minerals of P/T boundary in Meishan section, Changxin, Zhejiang province. Acta Sedimentol Sin 23:108–112, Chinese text with English abstract
12. Lu Q, Lei XR, Liu HF (1993) Study of the stacking sequences of a kind of irregular mixed-layer illite-smectite (I/S) clay mineral. Acta Geol Sin 67:123–130, Chinese text with English abstract
13. Wang SL (1998) The stacking type of I/S clays in the Permian-Triassic boundary stratigraphic sets of south China—a review. Northwestern Geol 19:14–19, Chinese text with English abstract

14. Hong HL, Xie SC, Lai XL (2011) Volcanism in association with the prelude to mass extinction and environment change across the Permian–Triassic boundary (PTB), southern China. Clays Clay Miner 59:478–489
15. Altaner SP, Ylagan RF (1997) Comparison of structural models of mixed-layer illite/smectite and reaction mechanisms of smectite illitization. Clays Clay Miner 45:517–533
16. Dong H, Peacor DR, Freed RL (1997) Phase relations among smectite, R1 illite-smectite, and illite. Am Mineral 82:379–391
17. Bauluz B, Peacor DR, Ylagan RF (2002) Transmission electron microscopy study of smectite illitization during hydrothermal alteration of a rhyolitic hyaloclastite from Ponza, Italy. Clays Clay Miner 50:157–173
18. Guizhou Bureau of Geology and Mineral Resources (1987) Regional Geological Annals of Guizhou Province. Beijing: Geological Publishing House, pp 698
19. Jackson ML (1978) Soil chemical analyses. Authors' publication University of Wisconsin Madison
20. Moore DM, Reynolds RC (1989) X-ray diffraction and the identification and analysis of clay minerals. Oxford University Press, Oxford, p 332
21. Islam AKME, Lotse EG (1986) Quantitative mineralogical analysis of some Bangladesh soils with X-ray, ion exchange and selective dissolution techniques. Clay Miner 21:31–42
22. Bronger A, Winter R, Sedov S (1998) Weathering and clay mineral formation in two Holocene soils and in buried paleosols in Tadjikistan: towards a Quaternary paleoclimatic record in Central Asia. Catena 34:19–34
23. Schwertmann U, Niederbudde EA (1993) Tonminerale in Böden. In: Jasmund K, Lagaly G (eds) Tonminerale und Tone, Struktur, Eigenschaften, Anwendung und Einsatz in Industrie und Umwelt. Steinkopff, Darmstadt, pp 212–265
24. Guthrie GD, Veblen DR (1989) High-resolution transmission electron microscopy of mixed-layer illite/smectite: computer simulations. Clays Clay Miner 37:1–11
25. Deconinck JF, Chamley H (1995) Diversity of smectite origins in late Cretaceous sediments: example of chalks from northern France. Clay Miner 30:365–379
26. Nieto F, Ortega-Huertas M, Peacor DR, Arostegui J (1996) Evolution of illite/smectite from early diagenesis through incipient metamorphism in sediments of the Basque-Cantabrian Basin. Clays Clay Miner 44:304–323
27. Brindley GW (1956) Allevardite, a swelling double-layer mica mineral. Am Mineral 41:91–103
28. Hong HL, Zhang XL, Wan M, Hou YJ, Du DW (2008) Morphological characteristics of K, Na-rectorite from Zhongxiang rectorite deposit, Hubei, central China. J China Univ Geosci 19:38–46
29. Środoń J (1984) X-ray powder diffraction identification of illitic materials. Clays Clay Miner 32:337–349
30. Schultz LG (1982) Mixed-layer illite/smectite and other minerals in shale, bentonite, and concretions in the Montana Disturbed Belt: Prog. Abst. 19th Annual Meeting, The Clay Minerals Society, Hilo, Hawaii, 1982, p 82 (abstract)
31. Murakami T, Inoue A, Lanson B, Meunier A, Beaufort D (2005) Illite-smectite mixed-layer minerals in the hydrothermal alteration of volcanic rocks: II. One-dimensional HRTEM structure images and formation mechanisms. Clays Clay Miner 53:440–451
32. Hower J, Eslinger EV, Hower ME, Perry EA (1976) Mechanism of burial metamorphism of argillaceous sediment: 1. Mineralogical and chemical evidence. Geol Soc Am Bull 87:725–737
33. Pearson MJ, Small JS (1988) Illite–smectite diagenesis and palaeotemperatures in northern North Sea Quaternary to Mesozoic shale sequences. Clay Miner 23:109–132
34. Reynolds RC, Hower J (1970) The nature of interlayering in mixed-layer illite-montmorillonite. Clays Clay Miner 18:25–36
35. Wang ZY (1998) Permian sedimentary facies and sequence stratigraphy in Daxiakou section, Xingshan county, Hubei province. J Jianhan Petrol Inst 20:1–7, Chinese text with English abstract

36. Chamley H (1989) Clay sedimentology. Springer, Berlin, p 623
37. Millot G (1970) Geology of clays. Springer, Berlin, p 499
38. Dera G, Pellenard P, Neige P, Deconinck JF, Pucéat E, Dommergues JL (2009) Distribution of clay minerals in Early Jurassic Peritethyan seas: Palaeoclimatic significance inferred from multiproxy comparisons. Palaeogeogr Palaeoclimatol Palaeoecol 271:39–51
39. Nadeau PH, Reynolds RC Jr (1981) Burial and contact metamorphism in the Mancos Shale. Clays Clay Miner 29:249–259
40. Pellenard P, Deconinck JF, Huff WD, Thierry J, Marchand D, Fortwengler D, Trouiller A (2003) Characterization and correlation of Upper Jurassic (Oxfordian) bentonite deposits in the Paris Basin and the Subalpine Basin, France. Sedimentology 50:1035–1060
41. Do Campo M, del Papa C, Nieto F, Hongn F, Petrinovic I (2010) Integrated analysis for constraining palaeoclimatic and volcanic influences on clay–mineral assemblages in orogenic basins (Palaeogene Andean foreland, Northwestern Argentina). Sediment Geol 228:98–112
42. Pearson MJ (1990) Clay mineral distribution and provenance in Mesozoic and Tertiary mudrocks of the Moray Firth and northern North Sea. Clay Miner 25:519–541
43. Meunier A, Lanson B, Velde B (2004) Composition variation of illite-vermiculite-smectite mixed-layer minerals in a bentonite bed from Charente (France). Clay Miner 39:317–332
44. Yin HF, Zhang KX, Tong JN, Yang ZY, Wu SB (2001) The global stratotype section and point (GSSP) of the 142 Hong et al. Clays and Clay Minerals Permian-Triassic boundary. Episodes 24:102–113
45. Wang GQ, Xia WC (2004) Conodont zonation across the Permian-Triassic boundary at the Xiakou section, Yichang city, Hubei province and its correlation with the Global Stratotype Section and Point of the PTB. Can J Earth Sci 41:323–330